Versatile Detector of Pseudo-periodic Patterns

Augusto Santini
Electronics Department (GIBIO)
National Technological University
Buenos Aires, Argentina
email: asantini@est.frba.utn.edu.ar

Emiliano Diez
Institute of Physiology, Medical School
National University of Cuyo
Mendoza, Argentina

Mariano Llamedo
Electronics Department (GIBIO)
National Technological University
Buenos Aires, Argentina
email: llamedom@frba.utn.edu.ar

***Abstract*—This study aimed to develop a detector with few physiologically-meaningful parameters, that could be capable of detecting pseudo periodic patterns. The algorithm is based in a signal detection based on a matched filter, and a threshold calculation based on robust statistics. The evaluation of the detector was performed under a corpus consisting in four sets. One set of human ECGs, one set of human PPG, one set of human Blood Pressure, and one set of rodent pseudo ECGs. The evaluation was performed with respect to the gold standard annotations, and was calculated in terms of sensitivity (S), positive predictive value (P) and F1 score (F). For the human ECG set of recordings, the detector had 99.9 S, 99.9 P and 99.9 F, for the human PPG set of recordings, the detector had 98.9 S, 99.2 P and 99.2 F, for the human Blood Pressure set of recordings, the detector had 100 S, 99.9 P and 99.9 F, while for the rodent pseudo ECG set of recordings the results where 100 S, 99.5 P and 99.8 F. All sets results are median values. The algorithm achieved promising results, in a broad set of recordings of very different nature.**

I. Introduction

The problem of cardiovascular diseases remains the leading cause of death on a global scale [1]. According to the World Health Organization, 17.9 million people died in recent years from cardiovascular disease, i.e 600,000 more people than the last report, representing 31% of global deaths.

The automatic analysis of pseudo periodic signals, such as those of cardiovascular origin, often relies on the detection of a synchronization pattern in order to perform a reliable estimation through averaging. In certain applications such as fetal ECG analysis or transmembrane action potential measurement, the automatic synchronization task can be a challenging problem by itself. The detections of heartbeats in the ECG can also be a challenging task, specially in those long-term and/or noisy recordings, with broad and sudden changes in rhythm and morphology. The success commonly relies on the *a priori* knowledge about the timing and morphologic description about the pattern to detect, therefore limiting the generality.

In the past two decades several cardiovascular pattern detectors were developed, e.g. ECG heartbeat detectors, blood pressure pulse detectors, etc. Some of them adapted for noninvasive signals such as the ECG or the plethysmographic signal, but also for other invasive signals, such as the electrogram and blood pressure recordings, among others. Several of the developed detectors are freely available on internet [2] and were described in the literature [3]. All the reviewed algorithms are commonly adapted to an specific type of pattern/signal, making difficult or impossible the possibility of changing the target pattern and/or signal. As a consequence, these algorithms have a limited adaptation capacity to real life applications, where noise interference and large morphological changes in the signal/patterns often occur. The objective of this work is to develop and analyze an algorithm to detect impulsive and pseudo periodic patterns in cardiovascular signals given a small set of timing and morphological constraints.

II. Methodology

A. ECG Databases

The performance of the algorithm was evaluated in a data corpus consisting in four evaluation datasets. The first evaluation set is constituted by 12 ECG databases, grouped into 5 categories: normal sinus rhythm (NSR), arrhythmia (AR), ST and T morphology changes (STT), stress (STR) and long-term (LT). Details of the human set are shown in Table I where only Lead II or the first available was selected for experimentation. All the databases have expert-reviewed QRS complex annotations, used as gold standard for the performance evalutaion. Overall, this evaluation set consists in 178 human ECG (hECG) recordings from 12 publicly available databases [2] [4], representing an exhaustive evaluation for QRS detectors.

Table I: Human evaluation set composition

Group	Name	Lenght	Rec	Leads
NSR	nsrdb	1 day	17	2
	fantasiadb	2 h	17	2-3
AR	mitdb	30 m	17	2
	svdb	30 m	17	2
	incartdb	30 m	17	12
STT	edb	2 h	17	2
	ltstdb	21 - 24 h	17	2-3
STR	thew	15 m	17	2
	stdb	20-40 m	17	2-3
LT	ltdb	14-22 h	7	2
	sddb	23 h	12	2
	ltafdb	1 day	17	2
Total		92 days	178	

In order to obtain an evaluation set that was not overpopulated with neither database, 17 random recordings where taken from the 12 different databases described in Table I except in the ones where the total recordings where less than 17, in which cases the whole databases where evaluated. The

algorithm was trained in a first evaluation set generated with this methodology, and finally evaluated in a second evaluation set created employing the same methodology.

B. Other cardiovascular signals

The second evaluation set consists in 5 human PPG recordings from the BIDMC [5] database, in which annotations where manually made for the PPG channel. The third evaluation set consists in 20 human blood pressure recordings from the 2014 Physionet/CinC Challenge [2] database, in which annotations where also manually made for the BP channel. The fourth evaluation set consists in 17 slices of pseudo ECG recordings, performed in explanted rodent hearts put through hipokalemia [6] where the signals taken where sliced in segments of approximately 1 minute in where both channels where stable and without significant morphological changes.

C. Algorithm Description

The algorithm proposed in this work is mainly based on the analysis of a detection signal calculated as

$$a(\theta) = \sum_{i=\theta}^{\theta+L-1} s(i).p(\theta - i) \quad , \quad \theta = 0, 1, ..., N \qquad (1)$$

where $p(n)$ (**p** hereafter) is a pattern of length N, and **s** the signal under analysis, of N samples length. This method is also known as the matched filter [3], where **p** is the time reversed version of the pattern to detect. The matched filter is the maximum likelihood delay estimator ($\hat{\theta}$) of a pattern **p** immerse in a signal **s** with additive uncorrelated Gaussian noise. One of the limitations can be that **p** must be known *a priori* for each subject, which is an important drawback at the moment of designing and automatic algorithm. In this work we proposed to overcome this limitation with the use of an arbitrary and fixed generic pattern **p**. The pattern has to be such that could match disruptive segments of the signal under analysis indicating that patterns are located in those locations of the signal, thus having a similar effect to a passband filter where the central frequency is dependent of the pattern width, as shown in Figure 1.

First the detection signal, **a** is calculated, using Equation 1 with a generic impulsive pattern calculated as

$$p(n) = g(n).\frac{\partial}{\partial n}.g(n)$$
$$g(n) = e^{-\frac{n^2}{2\sigma^2}} \quad , \quad \sigma = \frac{N-1}{5}$$

Note that the generic $p(n)$ is the derivative of a Gaussian pattern with a user-defined width N. The derivative was approximated by finite differences of the sequence $g(n)$. The detection signal a is then smoothed with an averaging low-pass FIR filter of integer length $M = 1.2 * N$, obtaining **a**. In the following block, all the maxima extreme values of **a** above a threshold $t_a = P_{30}\{\mathbf{a}\}$, are located and stored in

$$\mathbf{b} = \text{argmax}\{\mathbf{a} \geq t_a\}$$

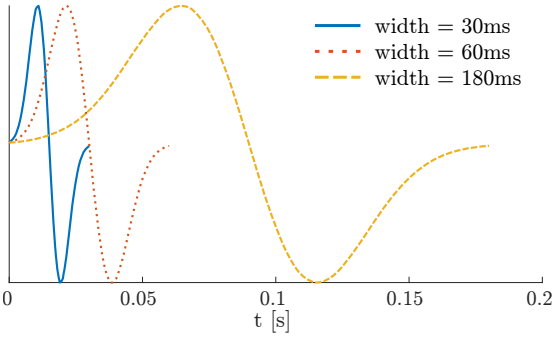

(a) Generic pattern time plot with normalized amplitude

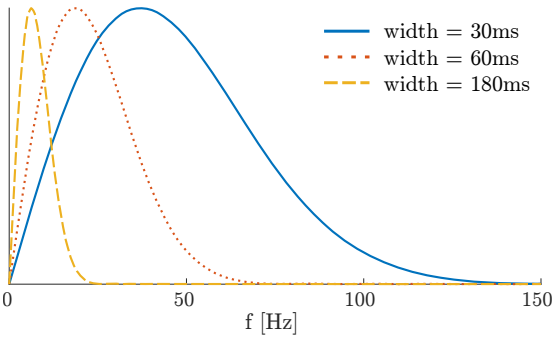

(b) Generic pattern frequency response with normalized amplitude

Figure 1: Generic pattern $p(n)$ and frequency response

The value of t_a was calculated as the 30th. percentile of **a**, and was empirically adopted in order to sample the noise floor. This algorithm is based on the assumption that the maximum values of the detection signal **a** where the pattern is not present will be significantly smaller than the ones where the pattern is present, thus making this difference a good metric to discern between pattern from non-pattern maximums. Another restriction required for the values of **b**, is that the occurrence of two subsequent maxima must be greater or equal than a user-defined parameter m_0, thus only the

$$b_j = \max_{n \in W}\{\mathbf{a}\}$$
$$W = \{j = 1, ..., B \wedge \forall k : b_k \geq (b_j + m_o)\}$$

are stored. Once all the B relevant extreme values are stored in **b**, the algorithm continues with the calculation of t_b, a second threshold used for the final impulse detection in signal **a**. The value of t_b is calculated from $\mathbf{h_b}$, i.e. the curve defined by the histogram values of **b**. The histogram was calculated by counting occurrences over an ad-hoc equally spaced grid, with a grid step calculated as

$$h_s = \text{med}\left\{\frac{\partial}{\partial l}e(l)\right\} \qquad (2)$$
$$e(l) = P_q\{\mathbf{b}\} \quad , \quad q = 1, 2, ..., 100 \qquad (3)$$

Note that h_s is the median finite difference of an uniformly sampled percentile grid over the values of **a**.

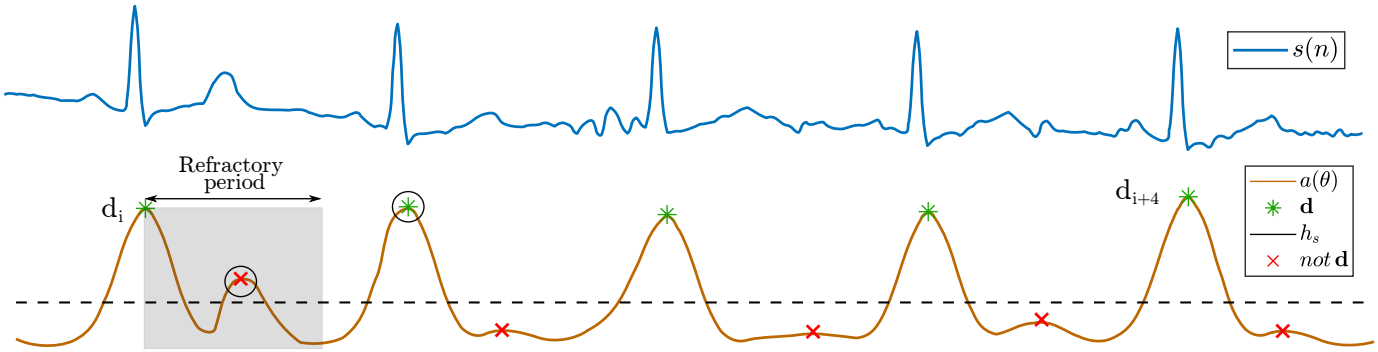

Figure 2: $s(n)$ and $a(\theta)$ with calculated threshold h_s and the detections $\mathbf{d}$. Note that the first of the two marked detections is discarded, even when it is above the calculated threshold value. This is due to the user defined temporal restriction between detections m_o.

The value of h_s favors an adequate representation of $\mathbf{h_b}$, in order to perform the calculation of the final detection threshold t_b which is calculated as the highest value that meets the conditions $h_b(t_b) = \min\{h_b\} \wedge t_b < \tilde{f}$, being $\tilde{f}$ calculated as:

$$\tilde{f} = \frac{\sum_{r=1}^{R} c(r).f(r)}{\sum_{r=1}^{R} c(r)}$$

with $c(r)$ being the local maxima of $\mathbf{h_b}$, being the points in which $\mathbf{h_b}'$ crosses zero, and $f(r)$ the indexes in which $c(r)$ occur.

Figure 3 shows $\mathbf{h_b}$ with different grids taken from the recording ltstdb/s20571 (lead 2). The detection process concludes after storing the Z_0 detections in

$$\mathbf{d} = (d_0, d_1, ..., d_{Z_0}) \quad , \quad d_z = \text{argmax}\{\mathbf{a} \geq t_b\}$$

The experimentation was performed with the user defined parameters in Table II.

Table II: Parameters used for the different sets

Set	m_o	N
Human ECG set	300ms	60ms
Human BP set	300ms	60ms
Human PPG set	300ms	180ms
Rodent ECG set	120ms	30ms

The evaluation of the proposed algorithm was performed with respect to the gold standard annotations included in each database. It was calculated by means of the sensitivity, positive predictive value and F score for each recording. The median results for each set of the corpus were calculated for a global performance assessment.

$$S = \frac{TP}{TP + FN}$$
$$P = \frac{TP}{TP + FP}$$
$$F = \frac{2TP}{2TP + FP + FN}$$

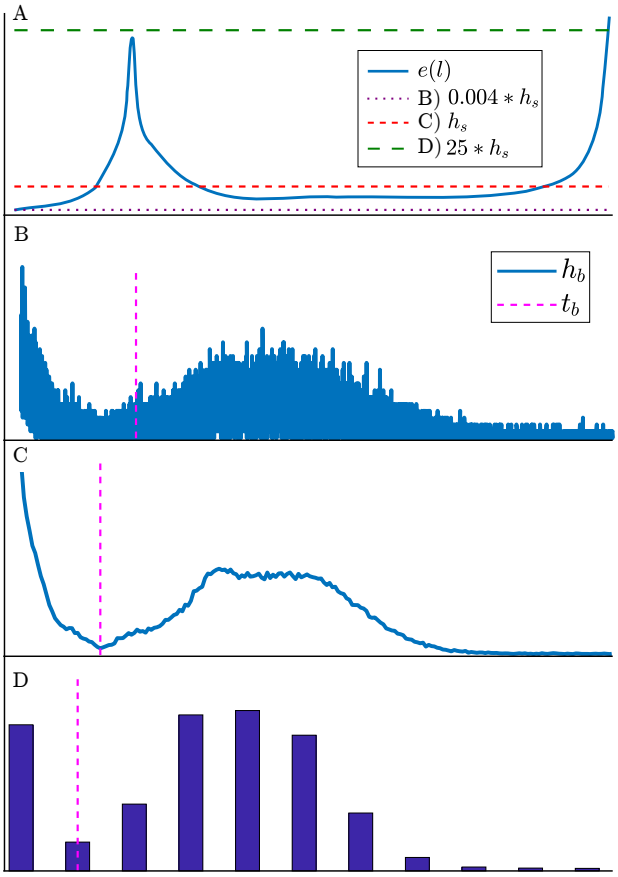

Figure 3: Effect of selecting several grid steps. In panel A, the percentile value sequence $e(l)$, and the calculated grid step for various example scales. From B to D the resulting histogram and the automatically calculated threshold t_b. The expected scenario C is achieved by calculating the grid step h_s from eq. 2

III. Results

The median results for the four sets are summarized in Table III.

Table III: Results for each set

Set	S	P	F
Human ECG	99.95	99.93	99.92
Human BP	100	99.86	99.89
Human PPG	98.87	99.18	99.17
Rodent ECG	100	99.55	99.78

The median results for the hECG set taking the MLII channel or the first channel if not found are compared with the 5th percentile with the same criterion and to the median results for the hECG set taking the best channel in each recording in Table IV.

Table IV: Results for the Human ECG set

Criteria	S	P	F
MLII or first lead	99.95	99.93	99.92
5th Percentile of MLII criterion	98.33	95.60	96.50
Best lead	99.96	99.95	99.95

To test the robustness of the algorithm against bad selections of the parameter N, in Table V are the results or the algorithm with different N only through the mitdb, with a fixed $m_0 = 300ms$.

Table V: Results for the mitdb with different N

N	S	P	F
30ms	99.908	99.899	99.893
60ms	99.904	99.951	99.919
120ms	99.894	99.936	99.904
180ms	99.700	99.936	99.748
240ms	98.146	99.786	97.901

A difference in the m_o parameter will result in the algorithm skipping patterns when m_0 turns too big, generating false negatives caused by the temporal restriction between patterns fixed by m_o.

IV. Discussion and Conclusions

In this work we evaluated an algorithm for the detection of pseudo-periodic patterns, such as the QRS complexes in the ECG. The pattern description was made with two time parameters: the pattern duration (N) and the minimum time between successive patterns (m_0). This algorithm was evaluated extensively in a broad set comprised of 178 human ECG (hECG) recordings of several types described in Table I. In order to evaluate the utility of the algorithm beyond hECG, three other datasets were included in the performance evaluation.

The hECG set in which the algorithm was evaluated included a wide variety of ECG types, as shown in Table I. The results achieved for the hECG set were $F = 99.92$, showing that the algorithm outperforms two publicly available detectors that are representative of the state of the art, i.e. *wavedet* [7] and *gqrs* [2] for the MLII criterion. The performance achieved was compared with an upper performance bound (UPB), defined as *best lead*, which consists in selecting the best performing lead for each recording. Note that this is not an achievable performance, since the correct pattern location is required beforehand. However, this UPB is useful to show the possibility of algorithm improvement, just by improving the lead selection criterion.

The algorithm was also evaluated in three additional dataset: 1) a blood pressure set where the performance achieved was $F = 99.89$, 2) a plethysmographic set, achieving $F = 99.17$ and finally 3) a rodent pseudo ECG set, where $F = 99.78$. As is shown, the performance achieved is in the order of the achieved for hECG, suggesting that the algorithm has certain ability to generalize adequately to data not considered during its development.

This versatility can be achieved with the two user-defined parameters m_0 and N. The effect of N is shown in Table V, showing the robustness of the algorithm in recordings where the width of the pattern under search is not an *a priori* knowledge or is uncertain. The effect of m_0 can be appreciated in Figure 2 in which is shown as the refractory period. In recordings where no time restriction between two patterns is needed or is not a known variable, this parameter can be zero, meaning that no pattern will be discarded for time restriction reasons.

We evaluated the computational cost of the algorithm and compare against two publicly available detectors, i.e *wavedet* and *gqrs*. In this evaluation we processed a single recording of 24 hours from the *ltafdb* [2] and measured the elapsed time. Our algorithm processed the recording in 189.9s, the *gqrs* in 97.53s and *wavedet* in 330.36s. The three algorithms where tested in the same computer and in the same recording for a fair comparison (ltafdb/114). Note that the *gqrs* is coded in C language while *wavedet* and our algorithm are implemented in MatLab (The Mathworks, Inc). The processing time achieved by our algorithm outperforms *wavedet* and gives better performance results, meaning that this algorithm has an acceptable computing performance.

The grid step calculated in equation 2 is needed for a good resolution of the histogram used in the algorithm and the final threshold calculation. The effect of several grid steps is shown in Figure 3 B-D. Note that situations B and D of this figure could result in a bad threshold calculation leading to the occurrence of false negatives and/or positives. However, in such scenarios, the algorithm is prepared to be assisted by an expert in the processing loop, correcting the automatically calculated threshold t_b, in order to achieve performances similar to the ones reported in this article. This situation, despite possible, did not happen in any of the evaluated recordings.

The implementation of the proposed algorithm with more detailed results can be found in [8] for comparison and to reproduce the results presented in this work. The algorithm achieved promising results in a broad set of recordings of very different nature, with a moderate computational cost, and with only two physiologically meaningful parameters. These features make the presented algorithm suitable for pattern detection in cardiovascular signals.

ACKNOWLEDGMENTS

This work was supported by projects ICUTNBA0004864 and ICUTNBA0004887 from UTN FRBA.

REFERENCES

[1] World Health Organization. (2012) Cardiovascular diseases. World Health Organization. [Online]. Available: http://www.who.int/cardiovascular_diseases/en/

[2] A. L. Goldberger *et al.*, "PhysioBank, PhysioToolkit, and PhysioNet: Components of a new research resource for complex physiologic signals," *Circulation*, vol. 101, no. 23, pp. e215–e220, 2000.

[3] L. Sörnmo and P. Laguna, *Bioelectrical Signal Processing in Cardiac and Neurological Applications*. Elsevier, 2005.

[4] J. P. Couderc. The telemetric and holter ECG warehouse initiative THEW. [Online]. Available: thew-project.org

[5] D. S. Baim, W. S. Colucci, E. S. Monrad, H. S. Smith, R. F. Wright, A. Lanoue, D. F. Gauthier, B. J. Ransil, W. Grossman, and E. Braunwald, "The bidmc congestive heart failure database," 2000. [Online]. Available: https://physionet.org/physiobank/database/chfdb/

[6] E. R. Diez *et al.*, "Melatonin, given at the time of reperfusion, prevents ventricular arrhythmias in isolated hearts from fructose fed rats and spontaneously hypertensive rats," *Journal of Pineal Research*, vol. 55, no. 2, pp. 166–173.

[7] J. P. Martínez, R. Almeida, S. Olmos, A. Rocha, and P. Laguna, "A wavelet-based ECG delineator: Evaluation on standard databases," *IEEE Transactions on Biomedical Engineering*, vol. 51, pp. 570–581, 2004.

[8] Implementation of the proposed algorithm. [Online]. Available: https://github.com/ajs93/aip.git